Experimental Investigations on The Effect of Tungsten Content on the Machining Behaviour of Tungsten Heavy Alloys

Chithajalu Kiran Sagar, Amrita Priyadarshini[*], and Amit Kumar Gupta

Mechanical Engineering Department, BITS-Pilani, Hyderabad Campus - 500 078, India
[*]E-mail: amrita@hyderabad.bits-pilani.ac.in

ABSTRACT

The present work attempts to assess the machinability of tungsten heavy alloys (WHAs) with varying tungsten content in terms of different machining variables under varied cutting conditions. It is observed that the feed rate has a significant effect on the machining characteristics, whereas the effect of rake angle appears to be marginal. With increase in W content both cutting force and material removal rate increase, whereas surface roughness decreases. Since WHAs are difficult to machine, an additional objective of the study is to optimise machining parameters. An optimal balance of the experimental cutting parameters using Grey relational analysis has been achieved, which can be effectively employed for the machining of the alloys with close dimensional tolerances and desirable surface finish.

Keywords: Tungsten heavy alloy; WHA; Machinability; Grey relation analysis

NOMENCLATURE

$\overline{G}$	Average particle size
V_W	Volume fraction of Tungsten
V_M	Matrix volume fraction
N_W	Number of tungsten particles
C_C	Contiguity
N_M	Number of matrix particles
N_{WW}	Number of W-W intercepts per unit length
N_{WM}	Number of W-matrix intercepts per unit length
MRR	Material removal rate
F_c	Cutting force
R_a	Surface roughness
W_i	Weight of work piece before machining
W_f	Weight of work piece after machining
t_m	Machining time
y_i	Experimental observed values for i^{th} experiment
k	Number of repeated trials for each ith factor
Y_{opt}	Optimum value of each output factor
$y_i^*(k)$	Analogous sequence
$y_i(k)$	Mean of repeated trials
$y_0^*(k)$	Reference sequence
$\delta_{i0}(k)$	Deviation sequence
δ_{max}	Maximum deviation sequence
δ_{min}	Minimum deviation sequence
χ	Discriminate coefficient
$\zeta_i(k)$	Grey relation coefficient
ψ_i	Grey relational grade for i^{th} experiment
γ_{pre}	Predicted grey relational grade
λ_i	Total mean grey relational grade
λ_0	Mean grey relational grade at optimum level

1. INTRODUCTION

Kinetic energy penetrators (KEPs), a class of weapons are extensively used in land-based warfare (Fig. 1). These weapons essentially use kinetic energy to destroy targets. The core of a KE penetrator is made up of a high-density material such as tungsten heavy alloy (WHA)[1,2]. Liquid phase sintering followed by swaging is a commonly used method for fabrication of these alloys[3,4]. Generally, the swaged tungsten alloy bars that form the cores of KEPs (10-30 mm diameter and 500-800 mm length) may develop non-uniform cross-section and poor surface finish[5]. Therefore, in order to get a desired finish/shape as well as a precise dimension, machining is necessary as a secondary operation. Turning operation imparts greater precision, especially with regards to features such as concentricity, roundness and thread details/dimension. Any stress concentration at the surface due to improper machining will lead to catastrophic failure during applications, especially in the case of KE penetrators. But precision machining with the desired surface finish can be challenging and uneconomical owing to the high strength, hardness and elastic modulus of the alloys.
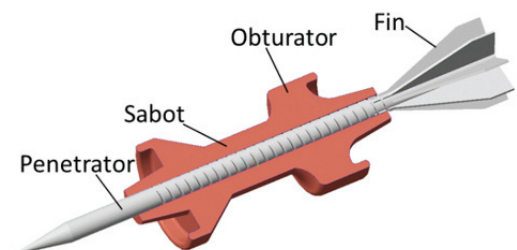

Figure 1. Isometric view of KEP.

Extensive studies have been found to evaluate the machinability based on a traditional approach that includes the assessment of chip morphology, cutting force, surface finish, tool life, and dimensional accuracy[6-10]. Advanced techniques such as polar diagram method[11], computational fluid dynamics[12] and block with disc using tribometer[13] may also be used. While considerable research has been directed towards understanding the machining characteristics of various difficult to cut alloys, detailed investigations on WHAs are scarce. Most of the efforts in this system have been made to understand the mechanical behaviour of WHAs that are influenced by tungsten content, type of processing and heat treatment[14,15]. However, not much of the research works are available that emphasize the machinability of various grades of WHAs[16,17]. Additionally, optimisation of the cutting variables has not been reported so far. Hence, there is a need to perform such assessments in WHAs while exploring the alloys as prospective materials for advanced KE penetrators that demand stringent dimensional control and excellent surface finish. In view of these requirements, the present paper focuses on the machinability assessments of three different grades of WHAs with varying tungsten content. Subsequently, attempts to find an optimal balance of machining parameters for a given grade of WHA using multi objective approach, namely Grey relation analysis, have been made.

2. EXPERIMENTAL DETAILS

The material for experimental investigation included WHAs containing 90, 95 and 97 (wt.%) W. The chemical composition, density and hardness of given WHAs was determined.

Standard procedures were used for microstructural evaluation that includes preparing the samples by cutting, mounting, grinding, polishing and etching (using Murakami's reagent for a time period of 30-60 seconds). The tungsten particle size, contiguity (W-W interfacial fraction) and volume fraction of the matrix phase of sintered WHAs were determined from images recorded using Scanning Electron Microscope (SEM) using mean chord intercept length, point counting method and counting W-W and W-M mean chord intercept line technique, respectively[18]. The Eqns (1), (2) and (3) are used for determination of microstructural parameters as listed below:

$$\overline{G} = \frac{2V_W}{2N_{WW} + N_{WM}} \quad (1)$$

$$V_M = \frac{N_M}{N_M + N_W} \times 100 \quad (2)$$

$$C_C = \frac{2N_{WW}}{2N_{WW} + N_{WM}} \times 100 \quad (3)$$

In order to study machinability, turning tests were conducted on a CNC lathe using uncoated cemented carbide tools. Before performing the machinability tests, the sintered and swaged WHA

sample alloys of length 130 mm were rough turned to a diameter of approximately 11 mm. All samples underwent heat treatment by heating the samples to 550 ˚C and then were held for about 4 hours for stress relief. The purpose is to reduce the internal stresses that might have developed in the work material due to swaging. The inert atmosphere was maintained during the heat treatment process by passing argon gas through a tubular furnace until the completion of the cycle[1]. The outputs, namely, machining force components, surface roughness and metal removal rate (MRR) and were measured during machining at varied cutting conditions. Each of the test conditions was repeated three times to ensure repeatability of the measured variables and consequently, mean values were reported. The experimental details are listed in Table 1 and the equipment used while conducting the machining trials are presented in Fig. 2.

Table 1. Experimental details of the machining tests

| Machine tool	CNC Lathe (HMT PTC200)
Tool holder	MCLNL2020K12, MSSNL2020K12
Tool Insert	CNMG120408, CNMA120408, SNMA120408
Tool rake angles (˚)	2, -5, -8
Nose radius (mm)	0.8
Cutting parameters	
Cutting velocity (m/min)	70, 50, 30
Feed (mm/rev)	0.05, 0.1. 0.15
Depth of cut (mm)	0.10, 0.15, 0.2
Length of cut (mm)	15
Tool cutting edge angles (˚)	80, 90
Cutting condition	Dry
Cutting force measurement	3- axis Piezoelectric lathe tool dynamometer
Surface roughness tester	Taylor Hobson precision profilometer
Microscope	Tool Maker's microscope Olympus-STM6
Weighing machine	Shimadzu AUW220 Analytical Balance
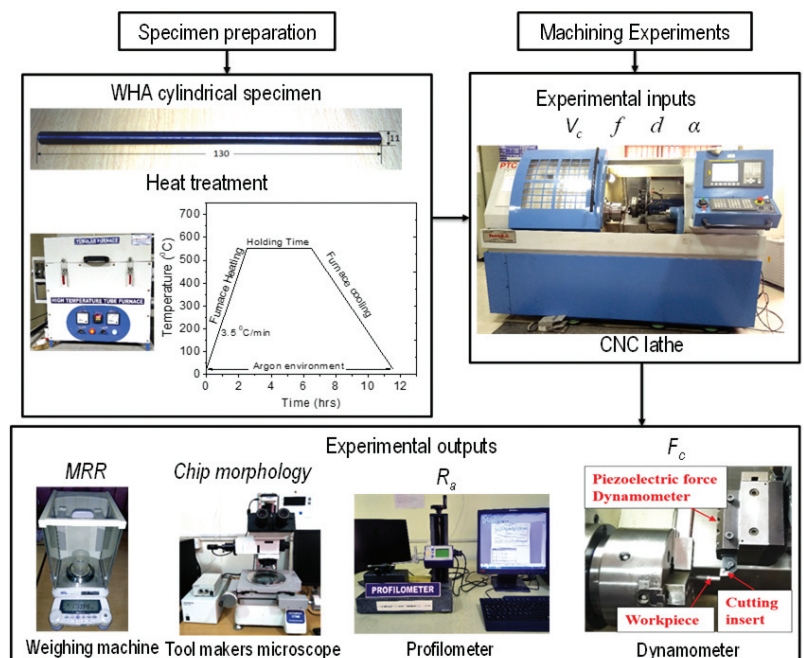
Figure 2. Experimental setup.

3. MICROSTRUCTURAL ANALYSIS AND MACHINABILITY STUDIES

The chemical composition as well as the values of density and hardness of 90, 95 and 97 WHAs are shown in Table 2. It is observed that both the density and hardness increase as the tungsten content increases.

3.1 Microstructural Analysis

Figure 3 shows the Scanning electron microscope images of 90, 95 and 97 WHA alloys. Different phases are labelled in the micrograph. In 90WHA, the W particles appear smaller and relatively more round in shape as compared to those in 95WHA and 97WHA. The particle size increases from 90 to 97WHA. The decrease in the volume fraction of the matrix as W content increases could be the probable reason for the difference in particle size. Also, as W increases, the particles become more angular. There is a process called shape accommodation that arises because of the decrease in volume fraction and an increase in W to ensure maximum packing. Such phenomena lead to planar interfaces and, thus, could be the basis of obtaining angular particles.

The contact area of the tungsten-matrix interface decreases and tungsten-tungsten interface increases with increasing W. A close observation was found by Islam[18], *et al.* when the tungsten content was increased from 88 WHA to 95 WHA. Fig. 4 clearly shows the increase of particle size, W-W contiguity and reduction in matrix volume fraction as the W content increases. The data points from the literature are superimposed[18]. The decrease in the volume fraction of the softer matrix would have led to an increase in hardness (Table 2). Such differences certainly have implications on the machining behaviour, which is discussed in the subsequent section.

3.2 Machinability Studies

The effect of tungsten content on machinability for WHAs has been investigated under different cutting conditions, namely, WHA grade, cutting parameters, tool rake angle. The chip morphology during the machining of alloys at variable cutting velocities for both negative and positive rake angles are presented in Fig. 5. Kindly note that tests were conducted at a constant feed rate and depth of cut of 0.1 mm/rev 0.15 mm, respectively. Machining using positive rake angle yields mixed type chips, i.e., discontinuous chips along with continuous type as compared to negative rake angle wherein the chips are the discontinuous type with only one exception that is in case of 90WHA. The difference is basically attributed to the material flow of work-piece in the region closer to the tool rake face. In general, for a negative rake angle, the material flow is unstable, resulting in cracks, especially in a brittle material. In contrast, when the rake angle is positive, shear deformation occurs, leading to bigger chips[19]. Since WHAs exhibit limited ductility, work-piece material undergoes limited plastic deformation with negative rake angle resulting in smaller chips. Hence, with the increase in W content, the tendency of

Table 2. Composition and physical properties of WHAs

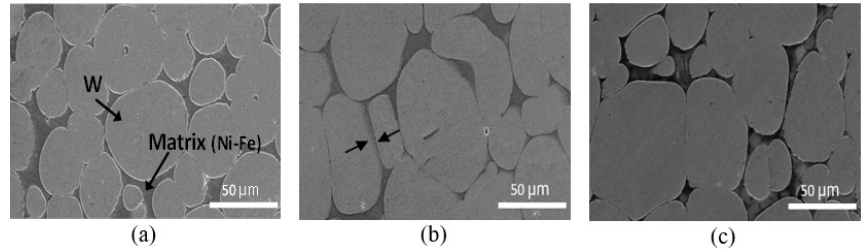| Grade	Composition				Density g/cc	Hardness	
	Fe (wt.%)	Ni (wt.%)	Co (wt.%)	W (wt.%)		HV	HRC
90WHA	2.5	5	2	90.5	17.0	294	29.8
95WHA	1.5	3	-	95.5	17.5	321	32.3
97WHA	1.5	2	-	96.5	18.1	330	33.3

Figure 3. Microstructural analysis of (a) 90 WHA (b) 95 WHA and (c) 97 WHA, arrows in (b) shows planar interface.
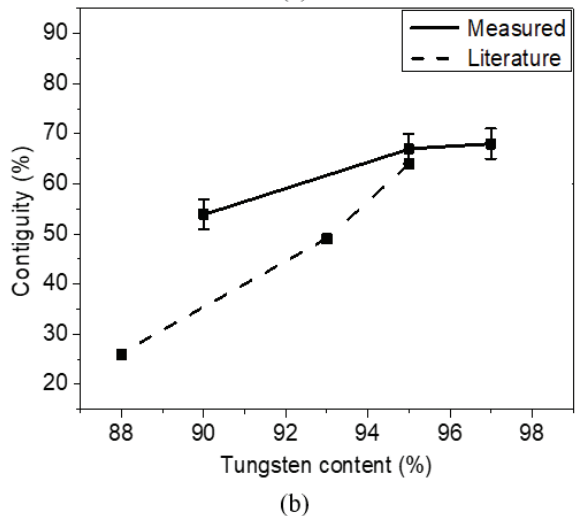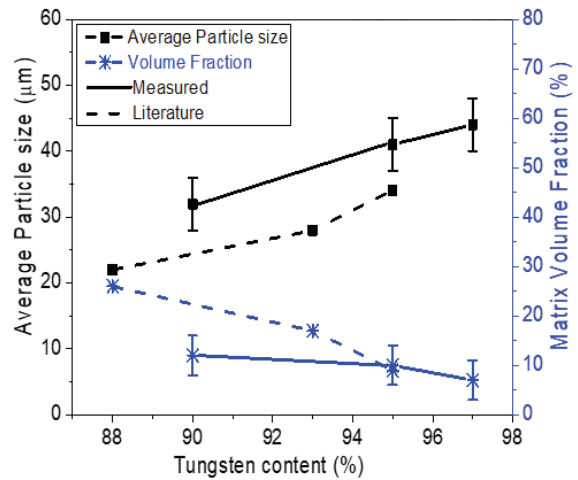

(a)

(b)

Figure 4. Comparison of observed (a) average particle size and matrix volume fraction and (b) contiguity as a function of tungsten content with the literature values[18].
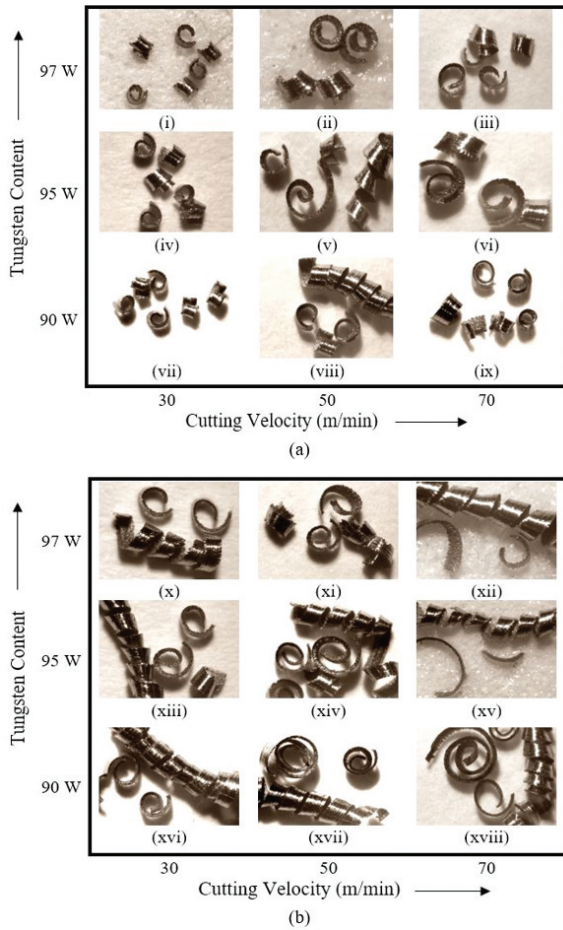
(a)

(b)

Figure 5. Chip morphology while machining WHAs using rake angle of (a) -5° and (b) 2° at cutting velocities of 30, 50 and 70 m/min.

chip fragmentation increases, which indicates increased brittle failure resulting in smaller chips. This may also be attributed to increasing contiguity that results in increasing brittleness as W-W interface is a potential crack nucleation site[20]. In case of a positive rake angle, a mixture of ductile and brittle failure gives rise to a mixed chip morphology.

MRR has been calculated experimentally and analytically using Eqns (4) and (5).

$$MRR_{Exp} = \left(\frac{W_i - W_f}{t_m} \right) \qquad (4)$$

$$MRR_{th} = V_c fd \qquad (5)$$

Figures 6 (a) and (b) show the variation of MRR with the change in cutting velocity and feed rate, respectively, for the given cutting tool geometries. All three grades of WHA show an increasing trend with the increase in cutting velocity and feed for both rake angles, except in one case. This is expected as per the metal cutting theory (Eqn (5)).

Figure 7 shows the change in cutting forces with respect to cutting velocity and feed rate. The cutting force versus cutting velocity for all grades show different trends for 2°and -5° rake angles. For the 2° rake angle, the cutting force decreases with increasing velocity, whereas no consistent trend is observed for the negative rake angle. The inconsistency in the trends could
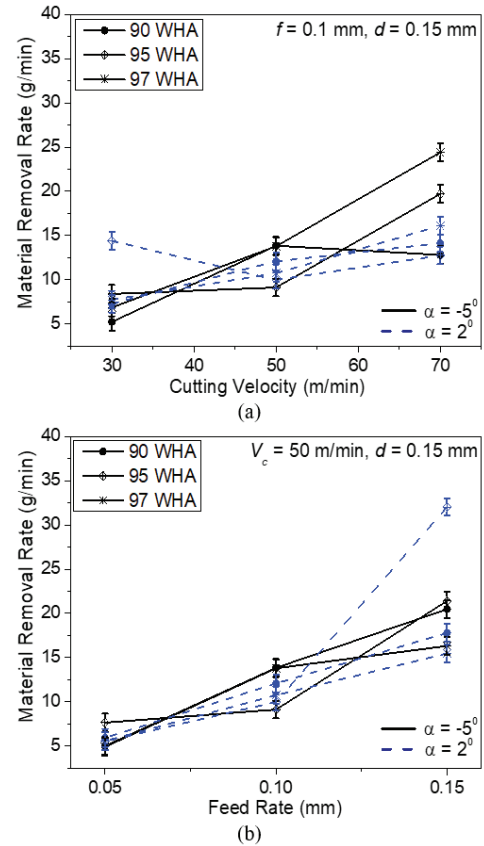

(a)

(b)

Figure 6. Change in MRR with respect to (a) cutting velocity and (b) feed rate.
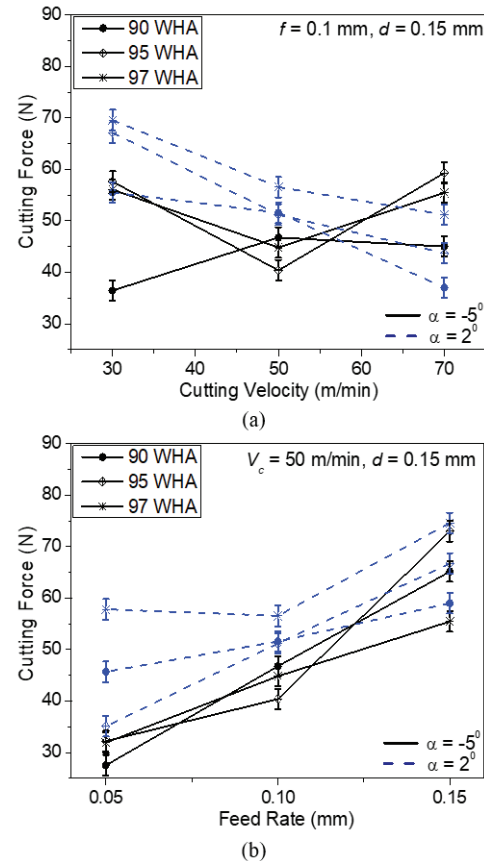

(a)

(b)

Figure 7. Change in cutting forces with respect to (a) cutting velocity and (b) feed rate.

165

occur due to brittle fragmentation that is statistical and prone to scatter.

For the lower cutting velocities, the values of cutting forces are higher for positive rake as compared to a negative rake angle. However, a cross over occurs at the highest velcoity (70 m/min.). This phenomenon could be correlated well with the type of chips being produced in the respective cutting conditions. The chips obtained using negative rake angle are discontinuous, producing small fragments due to brittle fracture, whereas, in the case of positive rake angle, chips are partly continuous type undergoing shear deformation. Since less force is required for removing smaller fragments, lower values of cutting force are observed in the case of a negative rake angle. The crossover at the highest velocity may be due to an additional parameter that is increasing temperature that may lead to material softening, which also explains the decrease in cutting force with increasing cutting velocity (for positive rake). The radius of curvature of chip curl could also be one probable factor for such a trend. It is observed smaller is the radius of curvature, more constricted is the curling of chips, thus increasing the compressive load on the tool, having a negative rake while removing the chips. The dependency of cutting force on feed rate is straightforward, i.e., increases with increasing feed rate.

It is noted that 97WHA exhibits higher values of cutting forces for positive rake angle with respect to both cutting velocity and feed. This may be due to the higher hardness value as observed in 97WHA. Owing to the predominantly brittle failure of the chips in case of negative rake angle, the hardness does not play a role and with scatter dominating, the trends are inconsistent for negative rake.
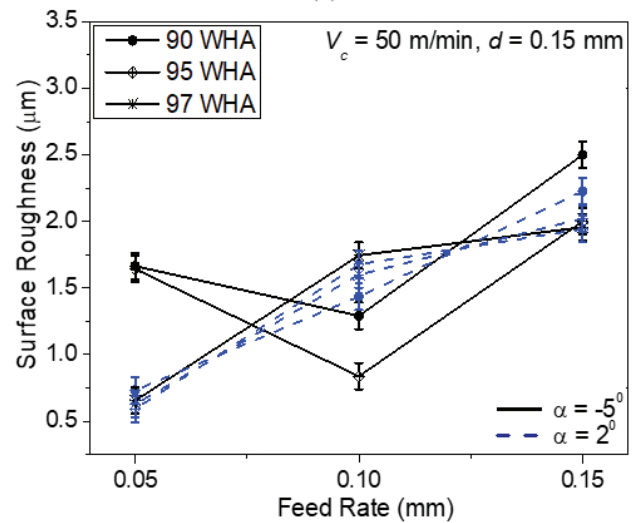
Similarly, change in surface roughness with repect to cutting velocity and feed rate is presented in Fig. 8. While for the positive angle, the roughness does not change much or at most exhibits a marginal decrease, no particular trend is seen for the negative rake angle. In the roughness versus feed plot, as the feed rate increases, roughness increases for the positive rake. However, the trends are found to be inconsistent for negative rake angle.

Figure 9 shows the change in surface roughness values with respect to cutting force for all three grades at variable cutting velocities and constant feed rate of 0.1 mm/rev. While the data are spread all over, a general trend is discernible, i.e., for negative and positive rake angle, the surface finish deteriorates with the increased cutting force values. The positive rake showed overall higher values for both cutting force and surface roughness as compared to that of the negative rake angle. It is observed that 90 WHA and 95 WHA at relatively lower cutting velocities showed the best possible values of surface roughness and cutting force, together, while 97 WHA showed the worst of all.

Furthermore, all three machining outputs have been plotted with respect to W content in Fig. 10. The increasing W content, leading to increased W-W contiguity, has significant implications on surface roughness, MRR and cutting force. On the whole, it can be inferred that with the increase in W content, MRR and cutting force increase considerably, but surface roughness does not change significantly, exhibiting a flat trend.
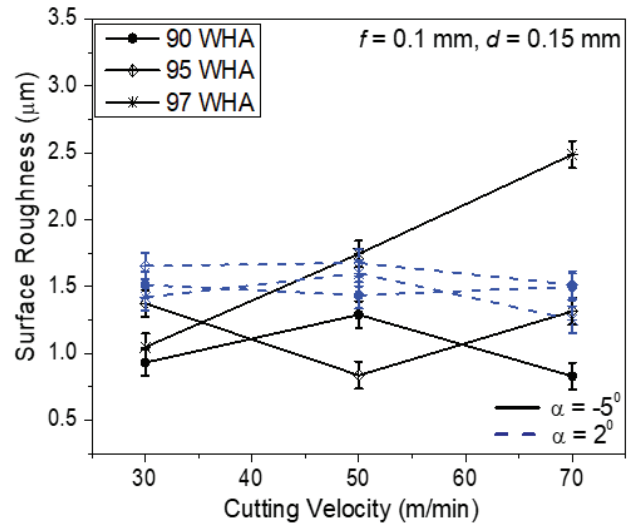
Figure 8. Change in surface roughness with respect to (a) cutting velocity and (b) feed rate.
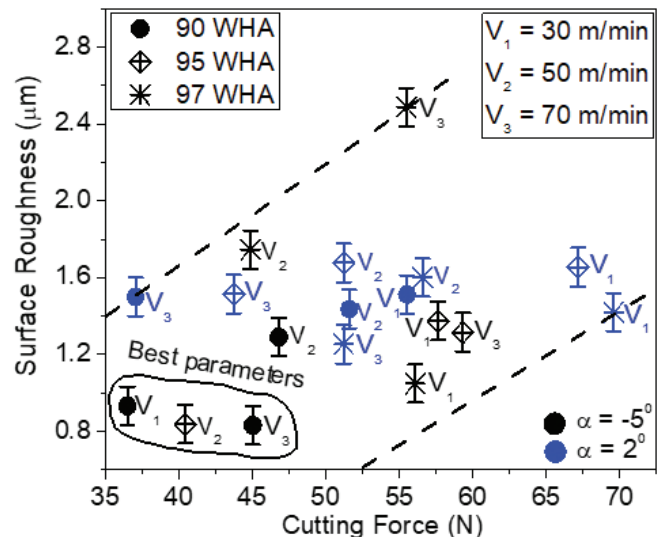

Figure 9. Change in surface roughness values with respect to cutting force under variable cutting velocities.
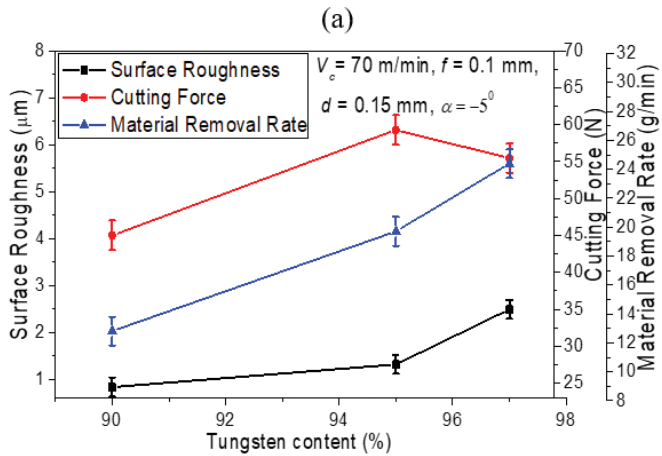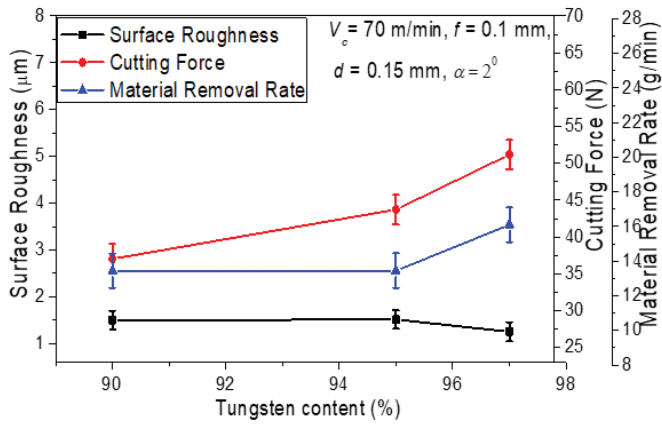
Figure 10. Effect of W content on surface roughness, cutting force, MRR for (a) positive and (b) negative rake angle.

4. MULTI-OBJECTIVE OPTIMISATION USING GRA

A comprehensive insight into the machinability of three different grades of WHAs under varied cutting conditions has been attained and hence, it can be stated that cutting parameters affect the machining outputs significantly. Consequently, there is a need to design the experiments in such a way that all the significant input parameters are taken into considerations for further analysis. This section focuses on developing a multi-objective optimisation model, using GRA, that would predict the right combinations of cutting parameters to achieve optimum machining variables, namely cutting force, surface roughness and MRR simultaneously[21,22]. Machining tests were conducted using the Taguchi L27 orthogonal array. Five input parameters, namely, Vc, f, d, α and G with three levels were considered. Table 3 (a) and (b) show the selected range of cutting parameters and the experimental design, respectively, considered for performing optimisation.

Figure 11 shows the flowchart depicting the major steps that have been followed to achieve the optimum output variables[21,22].

The experimental values, normalised mean, Grey relational coefficient and Grey relational grades (GRG) of response outputs F_c, R_a and MRR are presented in Table 4. The response outputs are normalised and converted to Grey relation coefficients as per steps 1, 2 and 3. GRGs are determined

Table 3. (a) Selected range of cutting parameters and (b) Experimental design

(a)

Symbol	Factors	Level		
		1	2	3
A	Cutting velocity (V_c)	30	50	70
B	Feed (f)	0.05	0.10	0.15
C	Depth of cut (d)	0.10	0.15	0.20
D	Rake angle (α)	-8	-5	2
E	Grade (G)	90	95	97

(b)

Exp. No.	V_c m/min	f mm/rev	d mm	α deg	G
1	30	0.05	0.20	-5	90
2	30	0.10	0.10	2	90
3	30	0.15	0.15	-8	90
4	50	0.05	0.15	2	90
5	50	0.10	0.20	-8	90
6	50	0.15	0.10	-5	90
7	70	0.05	0.10	-8	90
8	70	0.10	0.15	-5	90
9	70	0.15	0.20	2	90
10	30	0.05	0.20	-5	95
11	30	0.10	0.10	2	95
12	30	0.15	0.15	-8	95
13	50	0.05	0.15	2	95
14	50	0.10	0.20	-8	95
15	50	0.15	0.10	-5	95
16	70	0.05	0.10	-8	95
17	70	0.10	0.15	-5	95
18	70	0.15	0.20	2	95
19	30	0.05	0.20	-5	97
20	30	0.1	0.1	2	97
21	30	0.15	0.15	-8	97
22	50	0.05	0.15	2	97
23	50	0.1	0.2	-8	97
24	50	0.15	0.1	-5	97
25	70	0.05	0.10	-8	97
26	70	0.1	0.15	-5	97
27	70	0.15	0.2	2	97

by considering the mean of the Grey relational coefficients corresponding to each experiment combination as per step 4, as shown in Fig. 11.

Next, the GRG response is presented in Table 5. The listed values are calculated from the mean value of each input parameter associated with its corresponding level; for example, the mean of the GRG for $V_c = 30$ m/min is calculated by finding the average of the GRG for the experiments 1-3, 10-12 and 19-21. The optimum performance is then chosen based on the highest value of GRG for each parameter in Table 5. It is noted that the optimal machining parameters can be predicted using the estimated GRG using step 5 (see Fig. 11), which could be any value within the specified range and is not necessarily a value from the orthogonal array.

The optimum cutting parameter combination is found to be A1B2C1D2E2, i.e., cutting velocity, feed rate, rake angle and
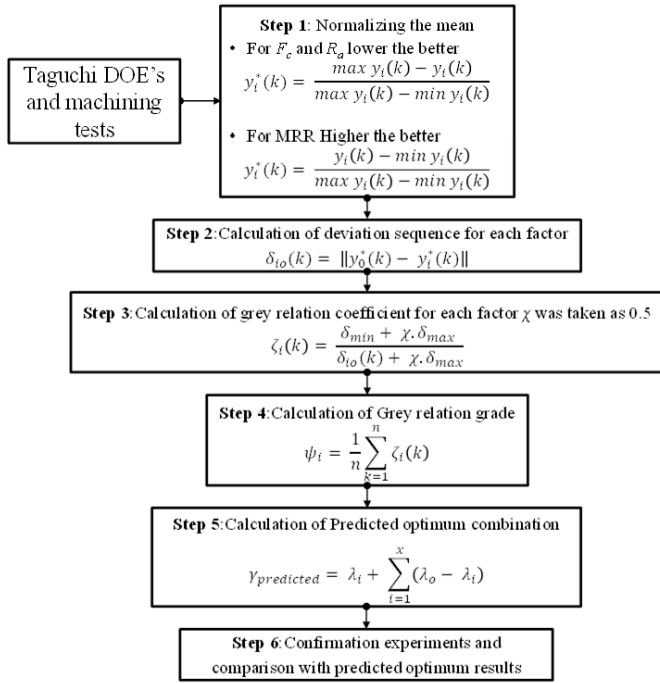
Figure 11. Flow chart for GRA.

Step 1: Normalizing the mean
- For F_c and R_a lower the better
$$y_i^*(k) = \frac{max\ y_i(k) - y_i(k)}{max\ y_i(k) - min\ y_i(k)}$$

- For MRR Higher the better
$$y_i^*(k) = \frac{y_i(k) - min\ y_i(k)}{max\ y_i(k) - min\ y_i(k)}$$

Step 2: Calculation of deviation sequence for each factor
$$\delta_{io}(k) = \|y_0^*(k) - y_i^*(k)\|$$

Step 3: Calculation of grey relation coefficient for each factor χ was taken as 0.5
$$\zeta_i(k) = \frac{\delta_{min} + \chi.\delta_{max}}{\delta_{io}(k) + \chi.\delta_{max}}$$

Step 4: Calculation of Grey relation grade
$$\psi_i = \frac{1}{n}\sum_{k=1}^{n}\zeta_i(k)$$

Step 5: Calculation of Predicted optimum combination
$$\gamma_{predicted} = \lambda_i + \sum_{t=1}^{x}(\lambda_o - \lambda_t)$$

Step 6: Confirmation experiments and comparison with predicted optimum results

Table 5. Response table for predicted optimum level based on GRG

Symbol	Cutting parameters	Grey relation grade			Mean effect
		Level 1	Level 2	Level 3	
A	Cutting velocity	**0.605**	0.567	0.575	0.081
B	Feed	0.604	**0.635**	0.555	0.055
C	Depth of cut	**0.615**	0.543	0.586	0.003
D	Rake angle	0.560	**0.609**	0.600	0.075
E	Grade	0.530	**0.583**	0.582	0.06

grade are 30 m/min, 0.1 mm/rev, 0.15 mm, -5°and 95 WHA, respectively. Furthermore, confirmation tests are conducted at the predicted optimum level of input parameters to determine the improvement of responses. It is noted that the confirmatory test are also repeated three times. Consequently, the resultant machining outputs are shown in Table 6. The results indicated that the value of predicted GRG (0.761) is closer to that of the experimental one (0.769).

Of all the grades, the best possible combination of cutting forces and surface roughness are found in the case of 95 WHA. Thus, it can be stated that 95WHA has better machinability among other WHA grades.

Table 4. Experimental results of different grades of WHAs and GRG

Exp. No.	F_c N	R_a μm	MRR g/min	Normalised mean			Grey relation co-efficient			GRG
				F_c	R_a	MRR	F_c	R_a	MRR	
1	46.40	1.14	4.72	0.646	0.801	0.047	0.585	0.715	0.344	0.548
2	33.23	1.30	3.98	0.829	0.740	0.025	0.746	0.658	0.339	0.581
3	68.80	2.28	6.19	0.333	0.373	0.091	0.428	0.444	0.355	0.409
4	44.58	0.78	6.48	0.671	0.936	0.100	0.603	0.887	0.357	0.616
5	57.26	1.16	14.47	0.494	0.793	0.339	0.497	0.707	0.431	0.545
6	76.61	1.78	12.94	0.224	0.561	0.293	0.392	0.533	0.414	0.446
7	21.02	0.89	4.86	1.000	0.894	0.051	1.000	0.825	0.345	0.724
8	44.97	1.02	12.52	0.666	0.847	0.280	0.599	0.766	0.410	0.592
9	86.17	2.10	24.45	0.090	0.443	0.637	0.355	0.473	0.579	0.469
10	45.11	0.76	5.00	0.664	0.944	0.055	0.598	0.900	0.346	0.615
11	34.42	0.90	3.15	0.813	0.889	0.000	0.728	0.819	0.333	0.627
12	71.00	2.23	6.62	0.302	0.393	0.104	0.417	0.451	0.358	0.409
13	32.88	0.85	4.13	0.834	0.910	0.029	0.751	0.847	0.340	0.646
14	55.02	0.92	18.15	0.525	0.883	0.449	0.513	0.811	0.476	0.600
15	79.45	1.24	10.10	0.184	0.763	0.208	0.380	0.678	0.387	0.482
16	23.36	3.07	6.50	0.967	0.078	0.100	0.939	0.352	0.357	0.549
17	51.81	1.11	19.45	0.570	0.812	0.488	0.538	0.726	0.494	0.586
18	86.20	1.91	36.58	0.090	0.511	1.000	0.355	0.506	1.000	0.620
19	47.32	0.64	5.57	0.633	0.987	0.072	0.577	0.975	0.350	0.634
20	32.33	0.82	3.15	0.842	0.922	0.000	0.760	0.865	0.333	0.653
21	68.43	2.12	7.10	0.338	0.435	0.118	0.430	0.470	0.362	0.421
22	45.91	0.61	5.21	0.652	1.000	0.062	0.590	1.000	0.348	0.646
23	60.05	1.06	15.63	0.455	0.831	0.373	0.478	0.748	0.444	0.557
24	69.82	1.23	9.77	0.319	0.767	0.198	0.423	0.682	0.384	0.496
25	22.62	3.28	6.23	0.978	0.000	0.092	0.957	0.333	0.355	0.549
26	55.71	2.01	18.08	0.516	0.476	0.447	0.508	0.488	0.475	0.490
27	92.63	1.80	23.40	0.000	0.553	0.606	0.333	0.528	0.559	0.474

Table 6. Comparison of cutting parameters between the predicted and experimental optimum levels

Parameters	Optimum cutting parameters	
	Predicted	Experiment
Level	A1B2C1D2E2	A1B2C1D2E2
F_c		26.23
R_a		0.91
MRR		8.16
Grey relational grade	0.761	0.769

5. CONCLUSIONS

The structure-property and machinability of 90, 95 and 97 WHA were investigated. There exists a strong relationship between tungsten content, microstructural parameters and hardness. This consequently affects the machinability aspects of WHAs with varying tungsten content. Chip morphology is found to be sensitive to tungsten content as well as cutting parameters, especially the tool geometry. The dependence of MRR, cutting force and surface roughness on feed rate and tungsten content show a clear trend but not in the case of cutting velocity. A complex interplay of different variables such as hardness, ductility/brittleness and temperature rise during machining appears to be responsible for such behaviour. Furthermore, Grey relation analysis was used for predicting the optimum machining variables. It can be observed that 95 WHA has better machinability as compared to 90 and 97WHAs. It is concluded that the optimum machining conditions predicted using GRA can be employed in precise machining of WHAs as an alternative to trial and error machining tests for the manufacture of KEPs that require stringent design tolerances.

REFERENCES

1. Das, J.; Rao, A.G.; Pabi, S.; Sankaranarayana, M. & Nandy, T.K. Thermo-mechanical processing, microstructure and tensile properties of a tungsten heavy alloy. *Mater. Sci. Eng. A*, 2014, **613**, 48-59.
   doi: 10.1016/j.msea.2014.06.072

2. Venkatesan, N. Recent Developments in Anti-Tank Ammunition. *Def. Sci. J.*, 1985, **35**(2), 225-230.
   doi: 10.14429/dsj.35.6015

3. Prabhu, G.; Kumar, A.K. & Nandy, T.K. Effect of yttrium oxide dispersion on the microstructure and properties of tungsten heavy alloys. *Def. Sci. J.*, 2018, **68**(4), 406-411.
   doi: 10.14429/dsj.68.12255

4. Liang, G.X. & Wang, E.D. Influence of hot extrusion on microstructure and mechanical properties of tungsten based heavy alloy. *J. Mater. Sci. Technol.*, 1996, **12**(12), 1032-1034.
   doi: 10.1080/02670836.1996.11665718

5. Dikshit, S. Ballistic behaviour of thick steel armour plate under oblique impact: Experimental investigation. *Def. Sci. J.*, 1998, **48**(3), 271-276.
   doi: 10.14429/dsj.48.3947

6. Zimmerman, C.; Boppana, S. & Katbi, K. Machinability test methods In: Metals Handbook, 9 ed., *ASM International*, 1989, 639-647. ISBN: 978-0-87170-022-3

7. Akdemir, A.; Yazman, S.; Saglam, H. & Uyaner, M. The Effects of Cutting Speed and Depth of Cut on Machinability Characteristics of Austempered Ductile Iron. *J. Manuf. Sci. Eng.*, 2012, **134**(2), 021013.
   doi: 10.1115/1.4005805

8. Veiga, C.; Davim, J.P. & Loureiro, A. Review on machinability of titanium alloys: the process perspective. *Rev. Adv. Mater. Sci.*, 2013, **34**, 148-164.

9. Umbrello, D.; Golpayegani, S. & Darak, Z. Experimental Investigation to Optimize Tool Life and Surface Roughness in Inconel 718 Machining. *Mater. Manuf. Process*, 2016, **31**(13), 1683-1691.
   doi: 10.1080/10426914.2015.1090592

10. Celik, A.; Yaman, H.; Turan, S.; Kara, A. & Kara, F. Effect of Heat Treatment on Green Machinability of SiAlON Compacts. *J. Mater. Process Tech.*, 2014, **214**, 767-774.
    doi: 10.1016/j.jmatprotec.2013.11.019

11. Rao, R.V. & Gandhi, O. Digraph and matrix methods for the machinability evaluation of work materials. *Int. J. mach. Tool Manu.*, 2002, **42**, 321-330.
    doi: 10.1016/S0890-6955(01)00133-X

12. Kundrak, J.; Gyani, K.; Tolvaj, B.; Palmai, Z.; Toth, R. & Markopoulos, A.P. Thermotechnical modelling of hard turning: A computational fluid dynamics approach. *Simul. Model. Pract. Theory*, 2017, **70**, 52-64.
    doi: 10.1016/j.simpat.2016.10.003

13. Lakic, G.G.; Borojevic, S.; Cica, D. & Sredanovic, B. Development of Aplication for Analysis of Machinability Index. *Tribol. Ind.*, 2009, **31**, 1-2.

14. Gurwell, W. Solid-state sintering of tungsten heavy alloys. *Mater. Manuf. Process*, 2007, **9**(6), 1115-1126.
    doi: 10.1080/10426919408934979

15. Pink, S.K. Deformation Mechanisms Operating in a Tungsten Heavy Alloy. *Mater. Sci. Eng. A*, 1997, **234-236**, 102-105.
    doi: 10.1016/S0921-5093(97)00201-3

16. Nandam, S.R.; Ravikiran, U. & Rao, A. A. Machining of tungsten heavy alloy under cryogenic environment. *Proc. Mater. Sci.*, 2014, **6**, 296-303.
    doi: 10.1016/j.mspro.2014.07.037

17. Sagar, C.K.; Kumar, T.; Priyadarshini, A. & Gupta, A.K. Prediction and optimization of machining forces using oxley's predictive theory and RSM approach during machining of WHAs. *Def. Technol.*, 2019, **15**(6), 923-935.
    doi: 10.1016/j.dt.2019.07.004

18. Islam, S.H.; Xuanhur, Q.U.; Askan, S.J.; Tufail, M. & Xinbo, H. Effect of microstructural parameters on the properties of W-Ni-Fe alloys. *Rare Met.*, 2007, **26**(3), 200.
    doi: 10.1016/S1001-0521(07)60201-0

19. Piispanen, V. Theory of formation of metal chips. *J. Appl. Phys.*, 1948, **19**(10), 876.
    doi: 10.1063/1.1697893

20. Rabin, B.H. & German, R.M. Microstructure effects on tensile properties of tungsten-Nickel-Iron composites. *Metall. Trans. A*, 1988, **19**(6), 1523-1532.
    doi: 10.1007/BF02674026

21. Ghetiya, N.D.; Patel, K.M. & Kavar, A.J. Multi-objective optimization of FSW process parameters of aluminium alloy using taguchi-based grey relational analysis. *T Indian I Metals*, 2016, **69**(4), 917-923.
doi: 10.1007/s12666-015-0581-1

22. Prakash, K.; Gopal, P. & Karthik, S. Multi-objective optimization using Taguchi based grey relational analysis in turning of Rock dust reinforced Aluminum MMC. *Measurement*, 2020, **157**.
doi: 10.1016/j.measurement.2020.107664

CONTRIBUTORS

Mr Chithajalu Kiran Sagar, obtained his MTech (Tool Engineering) from Rashtreeya Vidyalaya College of Engineering, Bengaluru, in 2012 and currently pursuing his PhD from Birla Institute of Technology and Science, Pilani – Hyderabad Campus. His research area: include material characterisation and machinability studies, finite element simulations and optimisation.

In the current study, he was instrumental in carrying out the experimental studies followed by detailed analysis as part of his PhD work.

Dr Amrita Priyadarshini, obtained her PhD from IIT Kharagpur, West Bengal, in 2012. Presently, she is working as Assistant professor at Department of Mechanical engineering, Birla Institute of Technology and Science, Pilani – Hyderabad Campus. Her areas of research includes: machinability studies, optimisation, finite element simulations, tribological studies.

In the present work, she has provided ideas and guidance for the analysis and documentation of results in the form of paper.

Prof. Amit Kumar Gupta, obtained his PhD from the School of Mechanical and Aerospace Engineering, Nanyang Technological University, Singapore, in 2006. He received the Singapore Millennium Foundation Scholarship Award (2002) for his doctoral study. He is Presently working as Professor in Mechanical engineering, Birla Institute of Technology and Science, Pilani – Hyderabad Campus. His research interest includes: operations research and management, production scheduling, simulation modelling of manufacturing systems, Sheet metal forming and optimisation.

In current study, he has provided guidance in performing the multi objective optimisation using Grey Relational Analysis.